TOROID-BASED CHARACTERIZATION OF CARDIAC DT-MRI

C. Mekkaoui[1], M. P. Jackowski[2], and A. J. Sinusas[1]

[1]Internal Medicine, Diagnostic Radiology, Yale University School of Medicine, New Haven, Connecticut, United States, [2]Dept. of Computer Science, Institute of Mathematics and Statistics, São Paulo, Brazil

Introduction

Diffusion Tensor Magnetic Resonance Imaging (DT-MRI) permits characterization of cardiac fiber structure and orientation **[1, 2]**. However, the complexity of the cardiac tissue architecture demands efficient strategies for visualization and analysis of tensor fields derived from cardiac DT-MRI. The purpose of this work is two-fold: ***(i)*** introduce a toroid-based representation of DT fields that improves myofiber visualization and ***(ii)*** define new diffusion scalar maps: the toroidal volume (**TV**) and the toroidal volume ratio (**TVR**) **[3]**. The methodology is applied on DT-MR images to characterize regions of tissue structure of a normal and infarcted canine hearts. Results indicate that the toroidal model improves myocardial structure characterization compared to ellipsoidal and superquadric **[4]** representations.

Methodology

***Toroid-based representation*:** The toroidal representation of the diffusion tensor is described by the parametric equation $\Im(\theta,\phi)=(\cos\theta(\alpha+\beta\cos\phi),\sin\theta(\alpha+\beta\cos\phi),\gamma\sin\phi)$, where $\Im$ is a function of both the azimuthal $\theta\in[0,2\pi]$ and polar $\phi\in[0,2\pi]$ coordinates. The parameters $\alpha=2\lambda_2+\lambda_3/4$, $\beta=\lambda_3/4$ and $\gamma=\lambda_1/2$ produce a subset of toroidal glyphs according to the local eigensystem. The toroid-based representation allows the creation of the toroidal volume map defined by $TV=(\pi/3)\lambda_1(\lambda_2\lambda_3+\lambda_3{}^2/2)$, which represents a measure of diffusivity. In addition, a new coefficient of anisotropy, the toroidal volume ratio (**TVR**) is defined by the ratio of the toroidal volume to the volume of a toroid scaled by $\langle\lambda\rangle$: $TVR=TV/TV_{\langle\lambda\rangle}$, $TV_{\langle\lambda\rangle}=\pi/2\langle\lambda\rangle^3$. These new indices provide complementary scalar maps representative of the tissue macrostructure. ***Data acquisition*:** After the animals were euthanized, hearts were excised and perfused with saline solution. Each heart was then placed and positioned in a container and filled with Fomblin (Ausimont, Thorofare, NJ). DT-MRI data were collected with a 3.0-T Siemens Trio scanner (Erlangen, Germany) using a segmented EPI sequence. An icosahedral diffusion encoding gradient scheme containing 6 directions was applied with a constant b-value=600 s/mm^2. A single image with a b-value=0 s/mm^2 was also obtained. Fifty short-axis image slices with resolution 2×2×2mm were acquired with TR=5400 ms and TE=84 ms. In order to increase SNR, a total of 32 averages were done and the EPI factor was set to 7, totaling 6 hours of acquisition time.

Results

The methodology was applied on the DT-MRI datasets of the normal heart and compared to the ellipsoidal and superquadrics representations. **Fig.1A** shows a short axis T2-weighted image at the mid-ventricles of a normal heart. **Fig.1B** shows the ellipsoidal and **Fig.1C** the superquadric representations in comparison with the toroidal glyph field (**Fig.1D**). The helical fiber pattern is easily identified with toroidal glyphs, but is more difficult to visualize with ellipsoids due to the lack of surface features. While superquadrics improve the characterization, this approach suffers from the same problem as the ellipsoids. Although they all reveal the orientation of the myocardial fibers, only toroidal glyphs appear to highlight the laminar architecture as depicted by the changing distribution of fiber angles from epicardium to endocardium (shaded area). **TV** and **{1-TVR}** maps were calculated for the infarcted heart and compared to **MD** and **{1-VR}** maps, respectively (**Fig.2**). The ischemic area is characterized by a substantial increase in **TV** indicating significant tissue alterations associated with myocardial infarction. In contrast, the infarcted regions demonstrate only a mild change in signal intensity on the **MD** map. The **{1-TVR}** map indicates a minor anisotropy reduction in the infarcted region which is consistent with loss of fiber structure and organization **[2]**. The distribution of reduced anisotropy cannot be easily identified in the **{1-VR}** map, because of the smaller range in the anisotropy values.

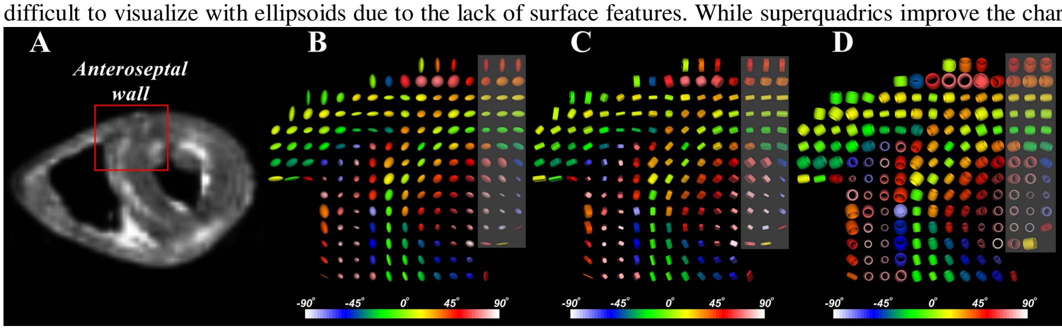

Fig.1 (**A**) Short-axis T2-weighted image of a normal canine heart. The ellipsoidal field is shown in (**B**), superquadrics in (**C**) and the toroidal glyph field in (**D**). Glyphs are colored according to the fiber inclination angle **[5]**.

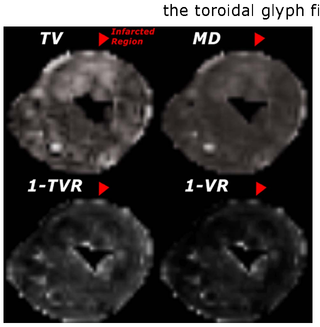

Fig.2 Top-row shows **TV** and **MD** maps of a mid-ventricular short-axis slice of an infarcted canine heart. Bottom-row shows the **{1-TVR}** and **{1-VR}** maps of the same slice.

Discussion

Characterization of cardiac tissue using DT-MRI relies on effective analysis and visualization methods. The toroid-based representation is less prone to visual ambiguity and concomitantly offers two new quantitative scalar maps that can potentially enhance the understanding of the underlying myocardial structure properties. The larger range of **TV** provides greater sensitivity for detection of subtle changes in diffusivity and **{1-TVR}** describes a degree of anisotropy which appears more sensitive than **{1-VR}**.

Conclusion

The increase in genus of the toroidal shape overcomes the lack of visual effectiveness in conventional representations of DT-MRI. In addition, the toroidal model provides new intrinsic indices represented by **TV** and **{1-TVR}**, which may complement traditional diffusion maps.

Acknowledgment: This study is sponsored by NIH grant HL078650 and a Brown-Coxe Fellowship to C.M. **References: [1]** LeGrice IJ *et al.* Am J Physiol 1995; 269:H571-82. **[2]** Helm PA *et al.* Circ Res 2006; 98:125-32. **[3]** Mekkaoui C *et al.* BMES 2007. **[4]** Ennis DB *et al.* Magn Reson Med 2005; 53:169-76. **[5]** Scollan *et al.* Am J Physiol 1998; 275:H2308-18.